Experimental Methods in Chemical Engineering: X-Ray Photoelectron Spectroscopy-XPS

Josianne Lefebvre,[1] Federico Galli,[2]* Claudia L. Bianchi,[2] Gregory S. Patience[3] and Daria C. Boffito[3]

1. Department of Engineering Physics, Polytechnique Montréal, C.P. 6079, Succ. CV Montréal, QC, H3C 3A7, Canada

2. Dipartimento di Chimica, Universitá degli Studi di Milano, via Golgi 19, 20133 Milano, Italy

3. Department of Chemical Engineering, Polytechnique Montréal, C.P. 6079, Succ. CV Montréal, QC, H3C 3A7, Canada

X-ray photoelectron spectroscopy (XPS) is a quantitative surface analysis technique used to identify the elemental composition, empirical formula, chemical state, and electronic state of an element. The kinetic energy of the electrons escaping from the material surface irradiated by an x-ray beam produces a spectrum. XPS identifies chemical species and quantifies their content and the interactions between surface species. It is minimally destructive and is sensitive to a depth between 1–10 nm. The elemental sensitivity is in the order of 0.1 atomic %. It requires ultra high vacuum (1×10^{-7} Pa) in the analysis chamber and measurement time varies from minutes to hours per sample depending on the analyte. XPS dates back 50 years ago. New spectrometers, detectors, and variable size photon beams, reduce analysis time and increase spatial resolution. An XPS bibliometric map of the 10 000 articles indexed by Web of Science[1] identifies five research clusters: (i) nanoparticles, thin films, and surfaces; (ii) catalysis, oxidation, reduction, stability, and oxides; (iii) nanocomposites, graphene, graphite, and electro-chemistry; (iv) photocatalysis, water, visible light, and TiO_2; and (v) adsorption, aqueous solutions, and waste water.

Keywords: depth profiling, nanocomposites, nanoparticles, photocatalysis, photoelectron peaks

INTRODUCTION

X-ray photoelectron spectroscopy (XPS) is a surface-sensitive quantitative analysis technique.[2] It probes the surface chemistry of materials and reports the elemental composition, empirical formula (without hydrogen), and chemical and electronic state of the elements, with an average analysis depth of 1–10 nm.[3] X-ray beams irradiating a material's surface generates a spectra of electrons with a characteristic kinetic energy. Each element produces a set of peaks at characteristic binding energies (the energy required to eject an electron from an atom and depends on the element, orbital, and chemical environment). The peaks refer to the electron configuration within the atoms, and the number of detected electrons (intensity) is related to how much is present. XPS software includes libraries of empirical or calculated relative sensitivity factors (RSF) for each element and each orbital and compute the element content from XPS peak areas. We calculate the atomic percentage on the surface layer based on the normalized corrected signals. The analysis chamber operates at a ultra-high vacuum (1×10^{-7} Pa) to minimize sample surface contamination and maximize the number of photoelectrons reaching the analyzer. It analyzes low vapour pressure solids such as inorganic compounds,[4] metal alloys,[5] semiconductors,[6] polymers,[7] elements,[8] catalysts,[9] glasses,[10] ceramics,[11] dry paints,[12] papers,[13] dry inks,[14] woods,[15] plant parts,[16] bones,[17] medical implants,[18] bio-materials,[19], glues,[20] soil particles,[21] and ion-modified materials.[22] It also analyzes some low vapour pressure liquids such as viscous oils[23] and ionic liquids.[24] In near-ambient pressure, XPS equipment can also analyze a variety of liquids and higher vapour pressure materials.[25]

This article reviews essential features of XPS and is part of a series that describes the most frequent analytical techniques, experimental methodologies, and statistical approaches in chemical engineering.[26,27] Together with some theory, it summarizes the science disciplines that apply this technique the most, highlights recent work published in *The Canadian Journal of Chemical Engineering*, and reports sources of error and uncertainties.

Description

A low-energy achromatic or monochromatic x-ray source (most often AlKα or MgKα) irradiates a sample in a ultrahigh vacuum, which ejects core-level electrons from the atoms (Figure 1). The kinetic energy of a photo-emitted core electron is a function of its binding energy in the atom and depends on the elements that compose the material. As a dominant relaxation mechanism at x-ray energies typical of XPS, an outer electron fills the formed core-hole and the emission of an Auger electron balances the transition energy. An electron energy analyzer and an electron detector count the emitted photoelectrons and Auger electrons as a function of their energy. The spectrum represents the material surface composition. The peak position on the energy scale refers to the element and the peak area indicates its relative amount.

*Author to whom correspondence may be addressed.
E-mail address: federico.galli@unimi.it
Can. J. Chem. Eng. 97:2588–2593, 2019

DOI 10.1002/cjce.23530
Published online 5 June 2019 in Wiley Online Library (wileyonlinelibrary.com).

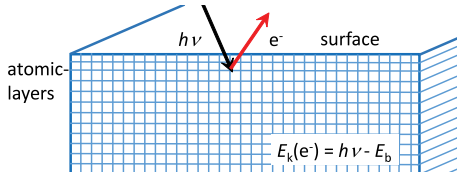

Figure 1. Solid surface electron emission. X-rays penetrate several atomic layers down to some μm; however, the top 2 to 3 layers contribute most to the spectra.

Only electrons from a maximum depth of 10 nm contribute to the signal, while a deeper electron emission contributes to the spectrum background. Even though the background is usually neglected, it contains information on sample structure.[28] Survey scans identify the elemental composition of 1 nm to 10 nm of the analyzed surface. High resolution spectra evaluate the chemical state of each element through a core electron binding energy shift of 8.0×10^{-20} J up to 8.0×10^{-19} J. Curve-fitting routines determine binding energies, which shift due to the atoms oxidation state, chemical bonds, or crystal structure. The tunable x-ray energy from synchrotrons radiation improves the photo-ionization cross-section for various elements and core levels.[29] Also, spectra with constant kinetic energy from synchrotron radiation ensures a constant and tunable information depth for all elements.[30]

Theory

When an electromagnetic wave hits a solid surface, the latter emits electrons, which is known as the photoelectric effect.[31] Metals absorb incident energy, which Einstein described as a corpuscle of energy hν; the material absorbs part of the energy ϕ (work function), while the residual is the kinetic energy (E_k) carried by the electron ($h\nu = \phi + E_k$)[32] (Figure 1).

Einstein's photoelectric effect (Figure 2) is the basis of photoelectron spectroscopy theory. Photons with an energy greater than the energy holding the electron in the atom ionize it. The excess energy transforms into electron kinetic energy.

Jenkin et al. recorded the photoelectron spectra of several metals.[33] Later, Siegbahn[34] included a high-resolution spectrometer to identify characteristic peaks of electrons in the shell and chemical bonding. Considering the energies before and after photoemission, the electron binding energy (E_b) is the difference between the ionized atom final energy state e (E_f) and the target atom initial energy state, (E_i) (Equations (1) and (2).

$$h\nu + E_i = E_k(e^-) + E_f \quad (1)$$

$$h\nu - E_k(e^-) = E_f - E_i = E_b \quad (2)$$

where E_k is the photoelectron kinetic energy.

Here we report a survey spectrum of a bimetallic catalyst of 10 % mass Fe and 10 % mass Co supported on alumina (FeCo, Figure 3).[35] A VG ESCALAB 3 MKII recorded the spectra. The x-ray source was Mg Kα. It operated at a power of 300 W and a spectrometer pass energy of 1.6×10^{17} J. The chamber pressure was 4×10^{-7} Pa and the electron takeoff angle between surface normal and entrance to energy analyzer was 0 rad. The analysis area was 2 × 3 mm. The Thermo Avantage v4.78 software quantified the survey results applying a homogeneous specimen model and Wagner sensitivity factors, after the charge correction

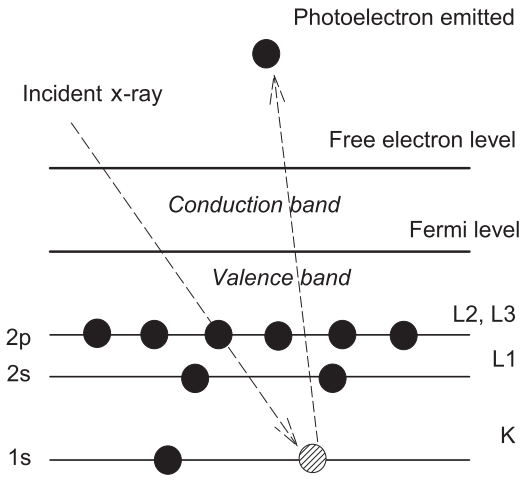

Figure 2. Photoelectric effect. In x-ray nomenclature, the 1st shell is designated as K ($n = 1$) that holds up to 2 electrons. The second shell is L ($n = 2$) with 2 + 6 electrons and the third shell is M ($n = 3$) with 2 + 6 + 10 electrons. The valence band is the outer shell of electrons and the conduction band.

of the C1s from adventitious carbon contamination to a binding energy of 4.6×10^{-17} J and background subtraction using a Shirley baseline. Quantification results were obtained from the Al2p, C1s, O1s, F1s, Fe2p3/2, and Co2p1/2 photoelectron peaks. We identified cobalt from the Co2p1/2 peak instead of the more typical Co2p or Co2p3/2 peaks because the Co2p3/2 peak overlaps with the O KLL peaks and using it will introduce errors in the quantification results.

APPLICATIONS

Industry professionals and academics apply XPS to study surface layers and thin films, nano-materials, photovoltaics, catalysis, corrosion, electronic devices and packaging, magnetic media, and coatings. In 2016 and 2017, over 18 000 articles indexed by WoS mentioned XPS,[26] and most of the articles appeared in physical chemistry with 3687 occurrences, followed by multidisciplinary materials science (2535), multidisciplinary chemistry (1578), chemical engineering (1515), and applied physics (1503). Chemical engineers publish articles most in the journals that specialize

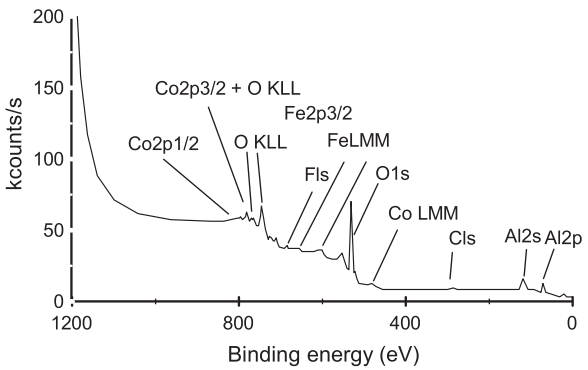

Figure 3. X-ray photoelectron survey spectrum obtained from a catalyst with a mass fraction of 10 % of both Fe and Co supported on alumina.

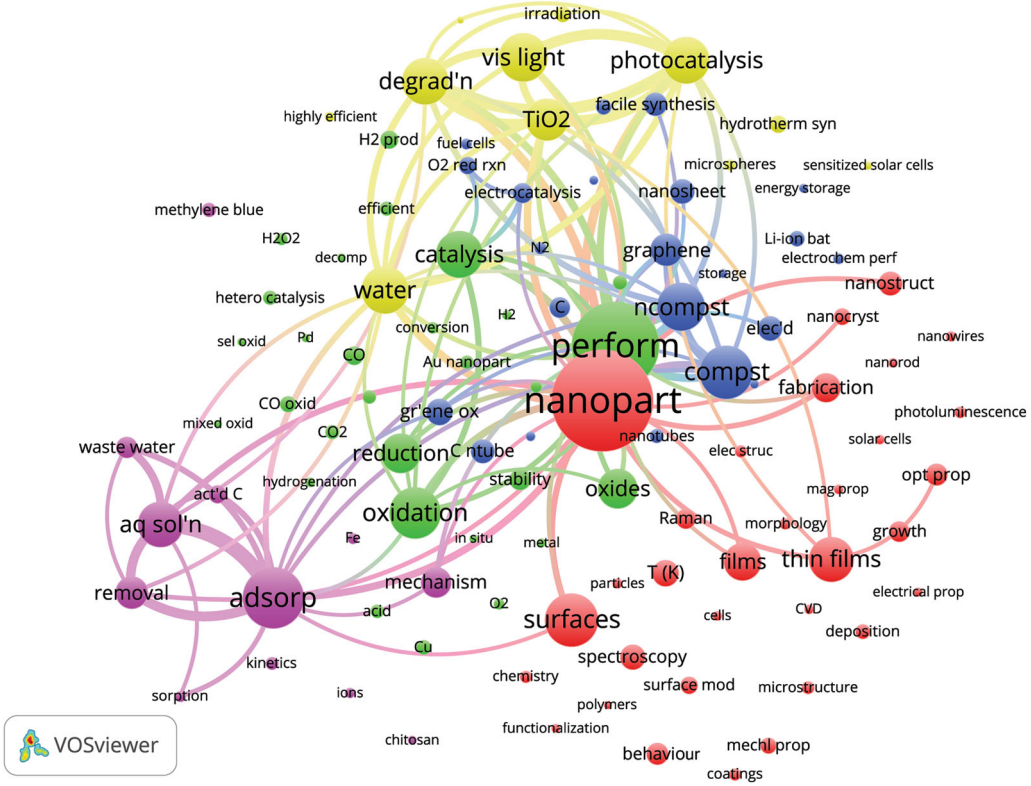

Figure 4. XPS bibliometric map of 107 keywords in the top 10 000 cited articles indexed by WoS in 2016 and 2017;[1,37] the VOSViewer groups keywords into 5 clusters (indicated by the colours), where the font size and circle size are proportional to the number of occurrences: nanoparticles appears in 1474 articles followed by performance (1268); adsorption (891); surfaces (775); and composites (774). The least frequent of the top 100 keywords appear less than 120 times: in situ (119); selective oxidation (118); mixed oxides (117); polymers (116); and sensitized solar cells (115). The lines represent citation links between articles.

in these WoS these categories.[36] Over 120 of the 252 WoS categories cite the technique at least once.

The VOSViewer software groups bibliometric data according to citation links and identified five major research clusters for XPS (Figure 4).[37] Nanoparticles, thin films, and surfaces are the most frequently cited keywords of the red cluster; it has 32 of the top 107 keywords. The green cluster has the second most number of keywords (29) and concentrates on catalysis: performance, oxidation, reduction, stability, and oxides. Nanocomposites, graphene, graphite, and electro-chemistry make up the keywords of the third ranked cluster (blue) with 22 keywords. The fourth cluster (yellow) includes photocatalysis, water, visible light, and TiO_2 and contains 12 keywords. The magenta cluster also has 12 keywords including adsorption, aqueous solutions, waste water, and removal. XPS analysis solves problems with existing surface interactions or investigates new materials. With respect to catalysis, it identifies features and changes related to both the active phase (transition metal particles, for example) and an inert support (alumina, metal oxides, TiO_2, zeolites, and carbon). XPS evaluates how the active component is dipsersed across the surface. For example, Mazzieri et al.[38] studied the properties of Ru/Al_2O_3 catalysts and XPS revealed Ru in RuO_3 or RuO_4 form and a decrease in the Ru/Al atomic ratios after calcination, which resulted from a migration of ruthenium species to the interior of the pellets.

Of the top 10 000 cited articles in WoS, *RSC Advances* published 695, followed by *Applied Surface Science* (657), *Journal of Alloys and Compounds* (307), *Applied Catalysis B-Environmental* (293), *Chemical Engineering Journal* (266), *Electrochimica Acta* (246), *ACS Applied Materials & Interfaces* (237), *Journal of Physical Chemistry C* (214), *International Journal of Hydrogen Energy* (191), *Ceramics International* (170), *Journal of Colloid and Interface Science* (9139), and *Catalysis Science & Technology* (134).

As of June 2018, the article entitled "n,p-Codoped Carbon Networks as Efficient Metal-Free Bifunctional Catalysts for Oxygen Reduction and Hydrogen Evolution Reactions" was cited 145 times.[39] The authors developed a 3D porous carbon network and included keywords from the blue and green clusters: electrocatalysis (blue); graphitic carbon (blue); hydrogen evolution (green); oxygen reduction (green); Zn air battery (blue); N_2 doped graphene (blue); electrocatalysis (blue); energy conversion; oxides (green); nanosheets (blue); nanotubes (blue); melamine; sheets; and water (yellow). The keywords in the second most cited article ("Advanced Electrochemical Energy Storage Supercapacitors Based on the Flexible Carbon Fiber Fabric-Coated with Uniform Coral-Like MnO_2 Structured Electrodes")[40] include MnO_2 nanostructures (red cluster), carbon fabric (blue), hydrothermal reaction (green), Li-ion batteries (blue), catalysis (green), high-performance (blue), fuel cells (blue), graphene (blue), nanotubes (blue), composites (blue), electro-catalysis (blue), and nanofibres (blue). In the 3rd most cited paper ("Macroscopic and Microscopic Investigation of U(VI) and Eu(III) Adsorption on Carbonaceous Nanofibers"),[41] the XPS and XANES analyses indicated that OH and COOH groups of the carbon nanofibres adsorbed the U(VI) and Eu(III). This research relates mostly to adsorption (magenta) and included sorption (magenta) and graphene oxide nanosheets (blue) among the keywords.

Can. J. Chem. Eng. published 33 articles in 2016 and 2017 that contained XPS among the keywords, which ranks it in the top third of all analytical techniques.[26] Feng et al.[42] investigated the features of ZnO/red clay sorbents. XPS characterized their surface properties before and after regeneration and established the chemical state of Zn, O, and S. Moreover, it showed that the surface was hydrated with water molecules and hydroxyl groups. Zuo et al.[43] prepared spherical supported catalysts, ZSM-5, γ-Al_2O_3, MCM-41, SBA-15, and β-zeolite, to produce methyl acrylate (MA) with phosphorous as the active component. The P2p peak intensity increased proportionally with the P loading until it reached the maximum feasible loading. Khalid et al.[44] investigated the gold dissolution from sulphidic minerals. XPS characterized the surface-obstructing species formed during the cyanidation process, and the single spectra of each metal disclosed the chemical state and composition responsible for the retarding effect on gold leaching. In the case of bimetallic catalysts, XPS reveals the electron transfer between metals and the consequent formation of an alloy,[45] as the binding energy of alloying is lower or higher than that of a standard pure species, proving that partial electron transfer occurred. Binding energy shifting also proved the decomposition from an oxidized species to new compounds. Ansaloni et al.[46] concluded that the Mo oxidation state was unaffected in the hydrodeoxygenation of guaiacol because the binding energies of the main peaks were unchanged after the reaction. Yang et al.[47] determined the chemical nature of the nitrogen-containing functional groups of activated carbon by XPS. Peak fitting revealed five nitrogen-containing species that are related to catalytic activity. Wang et al.[48] studied how additives changed the metal valence of Au and Cu ions on catalyst for the acetylene hydrochlorination at 165 °C by XPS.

UNCERTAINTY

Sources of Errors and Limitations

Sources of errors in an XPS experiment include mishandling specimens, contaminated vacuum condition in the XPS analysis chamber, specimen damage during the measurement, and questionable analytical strategies.[49] Strategies to limit surface contamination include handling specimens from edges with clean tweezers and avoiding direct contact of the surface region with anything, including gloves. Plastic containers transfer contaminants to the specimen surface such as plasticizers. Similarly, residues such as oils from the hand also contaminate the surface of a sample. Another unexpected source of contamination is demonstrated in the FeCo catalyst survey data (Figure 3), in which fluorine appears as a contaminant. The origin of this contamination is the PTFE coating of a magnetic stirrer when the operator prepared the sample.

XPS spectra are repeatable (precise) yet can be inaccurate. Statistical uncertainties in elemental quantification are ± 1 % or lower for large spectral peaks and greater for small peaks or noisy spectra. Systematic uncertainties reach 50 % in the worst case and contribute the most to inaccuracy, particularly due to applying an incorrect model. The peak area ratio (normalized by sensitivity factors) is the most common quantification method that assumes the sample is homogeneous, which is often erroneous for samples exposed to air because adventitious carbon contaminates the surface and/or a surface oxide layer forms. Furthermore, most samples are heterogeneous. Overlaying layers reduce the intensity of high binding energy peaks more than low binding energy peaks because the latter are from higher kinetic energy electrons that have a longer inelastic mean free path and thus are less attenuated traveling through the over layer. Recently, we analyzed homogeneous MoO_3 films and found that adventitious carbon contamination made up 30 % of the elemental composition of the analyzed volume. The calculated O/Mo ratio with the standard homogeneous analyte was 3:1 but the actual ratio was closer to 4:3 (based on XPS MultiQuant software that considers hydrocarbon contamination). Good practice requires researchers to determine the specimen morphology and to apply appropriate equations or models for quantification analysis.

Published XPS data and results also contain errors. Seldom do researchers evaluate uncertainties, and results are often reported with more significant figures than warranted considering experimental parameters. When researchers report the experimental conditions accurately, readers better assess the validity and quality of the results. High resolution XPS data are interpreted the majority of the time by producing a synthetic spectrum composed of a series of functions representing individual peaks. The sum of these peaks resembles the experimental spectrum. The analyst assigns to each of these individual peaks the chemical group or the oxidation state of the corresponding elemental spectra based on the peak's binding energy, with the help of previously published work or databases. This analysis is called peak fitting or curve synthesis (not deconvolution). XPS deconvolution methods calculate the energy loss spectrum from the original data or enhance spectral resolution by deconvoluting spectral broadening due to instrumental factors.

Case Study

Tables 1 and 2 compare systematic uncertainties to statistical uncertainties survey quantification results. The statistical uncertainty Δ_{mass} calculated from $N^{1/2}$ is negligible. For most peaks, the sample standard deviation s_{mass} determined from the five independent measurements is significantly larger. This is due to systematic uncertainty contributions. Even in the case where the same spot of the same sample is measured five times consecutively under the same conditions, there remains systematic uncertainty due to the choice of experimental parameters like step size while scanning the binding energy and data treatment by the analyst. In the case where five specimens of the same sample are analyzed (Table 2), the sample standard deviation is larger due to additional systematic uncertainty introduced from specimen positioning and, possibly, from differences between the specimens themselves, which occur if the catalyst sample is slightly heterogeneous. We also note that the relative standard deviation is larger for lower intensity peaks like C1s, F1s, Fe2p3/2, and Co2p3/2 even though they have a relatively low statistical uncertainty. We interpret this as being the result of additional uncertainty in

Table 1. XPS survey quantification results from five consecutive measurements of a single specimen with a mass fraction of 10 % of Fe and Co supported on alumina (x = mass fraction; Δ_{mass} = uncertainty; and s_{mass} = sample standard deviation)

Name	Atomic (%)	x (%)	Δ_{mass} (%)	s_{mass} (%)	s_{mass} (%) (relative)
Al2p	25.8	33.7	0.19	0.3	0.01
C1s	1.6	0.9	0.02	0.3	0.28
O1s	65.7	51.0	0.11	0.4	0.01
F1s	2.4	2.2	0.02	0.5	0.22
Fe2p3/2	2.1	5.7	0.04	0.3	0.05
Co2p1/2	2.5	6.5	0.06	0.6	0.09

Table 2. XPS survey quantification results from the measurement of five different specimens of a sample with a mass fraction of 10 % of Fe and Co supported on alumina

Name	Atomic (%)	x (%)	Δ_{mass} (%)	s_{mass} (%)	s_{mass} (%) (relative)
Al2p	25.3	33.3	0.18	0.6	0.02
C1s	2.0	1.1	0.02	0.5	0.46
O1s	66.1	51.7	0.11	1.1	0.02
F1s	2.4	2.2	0.02	0.3	0.11
Fe2p3/2	2.0	5.4	0.04	0.4	0.07
Co2p1/2	2.2	6.2	0.06	0.8	0.13

determining the limits of the peaks in data treatment for low intensity peaks compared to higher intensity peaks.

The experimental uncertainty calculated from the standard deviation from five repeated measurements does not provide much information about the accuracy of the quantification results. Indeed, we applied a homogeneous quantification model, while the specimens studied are actually far from homogeneous in the analysis volume. We might be able to model them as alumina spheres with islands of Fe and Co on the surface, however, this would still be innacurate as the surface of alumina is rough and porous. This example shows that, in XPS analysis, accuracy is easy to obtain and quantify, though good repeatability and precision in addition to chemical state identification make it an interesting technique to compare samples.

CONCLUSIONS

XPS analysis identifies elements or chemical groups based on binding energy at which photoelectron peaks are detected. We deduce elemental content from the area of the peaks. The choice of suitable experimental parameters and acquisition of spectra with adequate signal to noise ratio minimizes uncertainties. Accuracy improves by choosing an appropriate quantification model. Recent commercial XPS systems perform depth profiling on a variety of materials including organics with new ionic species for etching and chemical state imaging to a spatial resolution down to 3 μm. New higher energy monochromatic x-ray sources such as AgLα are also available, which increase the information depth and create opportunities for non-destructive depth profiling surface layers. Synchrotron radiation is the best x-ray source for XPS because the monochromatic beam produces a narrower peak and, therefore, reduces peak overlap. For example, the Ru $3d_{5/2}$ and Ru $3d_{3/2}$ binding energy of Ru metal is 4.49×10^{-17} J and 4.55×10^{-17} J, respectively, and 4.50×10^{-17} J and 4.57×10^{-17} J, respectively for Ru^{4+}, while it is 3.98×10^{-17} J for carbon. With standard commercial Al anodes, the C1s peak with a maximum at 4.56×10^{-17} J and a width of 1.6×10^{-19} J at half the peak height, overlaps with the Ru3d peaks. This leads to increased uncertainty in the quantification of these elements.

REFERENCES

[1] Clarivate Analytics, *Web of Science Core Collection*, accessed on 25 June **2018**, http://apps.webofknowledge.com.

[2] J. D. Andrade, "X-ray Photoelectron Spectroscopy (XPS)," *Surface and Interfacial Aspects of Biomedical Polymers: Surface Chemistry and Physics*, Joseph D. Andrade, Ed., Springer Science & Business Media, New York **2012**, 105–195.

[3] B. D. Ratner, D. G. Castner, "Electron Spectroscopy for Chemical Analysis," *Surface Analysis: The Principal Techniques*, J. C. Vickerman, I. S. Gilmore, Eds., John Wiley & Sons, Hoboken **2011**, 47–113.

[4] L. Cizaire, B. Vacher, T. L. Mogne, L. Cizaire, B. Vacher, T. L. Mogne, J. Martin, L. Rapoport, A. Margolin, R. Tenne, *Surf. Coat. Tech.* **2002**, *160*, 282.

[5] A. Aric, A. Shukla, H. Kim, S. Park, M. Min, V. Antonucci, *Appl. Surf. Sci.* **2001**, *172*, 33.

[6] E. A. Kraut, R. W. Grant, J. R. Waldrop, S. P. Kowalczyk, *Phys. Rev. Lett.* **1980**, *44*, 1620.

[7] G. Beamson, D. Briggs, *High Resolution XPS of Organic Polymers: The Scienta ESCA300 Database*, Wiley, Hoboken **1992**.

[8] J. Moulder, J. Chastain, *Handbook of X-ray Photoelectron Spectroscopy: A Reference Book of Standard Spectra for Identification and Interpretation of XPS Data*, Physical Electronics Division, Perkin-Elmer Corporation, Eden Prairie **1992**.

[9] K. R. Priolkar, P. Bera, P. R. Sarode, M. S. Hegde, S. Emura, R. Ku-Mashiro, N. P. Lalla, *Chem. Mater.* **2002**, *14*, 2120.

[10] A. Mekki, D. Holland, C. McConville, M. Salim, *J. Non-Cryst. Solid.* **1996**, *208*, 267.

[11] J. Das, S. Pradhan, D. Sahu, D Mishra, S. Sarangi, B. Nayak, S. Verma, B. Roul, *Physica B* **2010**, *405*, 2492.

[12] C. Altavilla, E. Ciliberto, *Appl. Phys. A-Mater.* **2004**, *79*, 309.

[13] S. Chen, H. Tanaka, *J. Wood Sci.* **1998**, *44*, 303.

[14] J. Dalton, J. Preston, P. Heard, G. Allen, N. Elton, J. Husband, *Colloid. Surface. A* **2002**, *205*, 199.

[15] G. N. Inari, M. Petrissans, J. Lambert, J. J. Ehrhardt, P. Grardin, *Surface Interface Anal.* **2006**, *38*, 1336.

[16] T. Hietala, N. Mozes, M. J. Genet, H. Rosenqvist, S. Laakso, *Colloid. Surface. B* **1997**, *8*, 205.

[17] A. M. Arroyo, M. L. Ruiz, G. V. Bernabeu, R. S. Román, M. G. Morales, L. Straus, *J. Archaeol. Sci.* **2008**, *35*, 801.

[18] Y. Okazaki, Y. Ito, K. Kyo, T. Tateishi, *Mat. Sci. Eng.-A Struct.* **1996**, *213*, 138.

[19] B. Nisol, S. Watson, A. Meunier, D. Juncker, S. Lerouge, M. R. Wertheimer, *Plasma Process. Polym.* **2018**, *15*, 1700132.

[20] G. Z. Xiao, M. Delamar, M. Shanahan, *J. Appl. Polym. Sci.* **1997**, *65*, 449.

[21] W. Amelung, K. Kaiser, G. Kammerer, G. Sauer, *Soil Sci. Soc. Am. J.* **2002**, *66*, 1526.

[22] K. Sahre, K.-J. Eichhorn, F. Simon, D. Pleul, A. Janke, G. Gerlach, *Surf. Coat. Tech.* **2001**, *139*, 257.

[23] T. Mundry, P. Surmann, T. Schurreit, *Fresenius' Journal of Analytical Chemistry* **2000**, *368*, 820.

[24] O. Hfft, S. Bahr, M. Himmerlich, S. Krischok, J. A. Schaefer, V. Kempter, *Langmuir* **2006**, *22*, 7120.

[25] S. Kaya, H. Ogasawara, L. Kenslund, J.-O. Forsell, H. S. Casalongue, D. J. Miller, A. Nilsson, *Catal. Today* **2013**, *205*, 101.

[26] G. S. Patience, *Can. J. Chem. Eng.* **2018**, *96*, 2312.

[27] G. S. Patience, *Experimental Methods and Instrumentation for Chemical Engineers*, 2nd edition, Elsevier, Amsterdam **2017**.

[28] S. Hajati, S. Tougaard, *Journal of Surface Analysis* **2009**, *15*, 220.

[29] D. Briggs, M. Seah, *Practical Surface Analysis: By Auger and X-ray Photo-Electron Spectroscopy*, Wiley, Chichester, PA **1983**.

[30] P.-L. Girard-Lauriault, T. Gross, A. Lippitz, W. E. Unger, *Anal. Chem.* **2012**, *84*, 5984.

[31] H. Bonzel, C. Kleint, *Prog. Surf. Sci.* **1995**, *49*, 107.

[32] O. W. Richardson, K. T. Compton, *The London, Edinburgh, and Dublin Philosophical Magazine and Journal of Science* **1912**, *24*, 575.

[33] J. Jenkin, R. Leckey, J. Liesegang, *J. Electron Spectrosc.* **1977**, *12*, 1.

[34] K. Siegbahn, *Ark. Fys.* **1954**, *7*, 86.

[35] P. Louyot, C. Neagoe, F. Galli, C. Pirola, G. S. Patience, D. C. Boffito, *Ultrason. Sonochem.* **2018**, *48*, 523.

[36] G. S. Patience, C. A. Patience, F. Bertrand, *Can. J. Chem. Eng.* **2018**, *96*, 811.

[37] N. J. Van Eck, L. Waltman, *Scientometrics* **2010**, *84*, 523.

[38] V. Mazzieri, F. Coloma-Pascual, A. Arcoya, P. LArgentire, N. Fígoli, *Appl. Surf. Sci.* **2003**, *210*, 222.

[39] J. Zhang, L. Qu, G. Shi, J. Liu, J. Chen, L. Dai, *Angew. Chem. Int. Edit.* **2016**, *55*, 2230.

[40] M. Cakici, K. R. Reddy, F. Alonso-Marroquin, *Chem. Eng. J.* **2016**, *309*, 151.

[41] Y. Sun, Z.-Y. Wu, X. Wang, *Environ. Sci. Technol.* **2016**, *50*, 4459.

[42] Y. Feng, Y. Li, L. Shi, M. Wu, J. Mi, *Can. J. Chem. Eng.* **2017**, *95*, 2087.

[43] C. Zuo, C. Li, T. Ge, X. Guo, S. Zhang, *Can. J. Chem. Eng.* **2017**, *95*, 2104.

[44] M. Khalid, F. Larachi, A. Adnot, *Can. J. Chem. Eng.* **2017**, *95*, 1875.

[45] F. Li, J. Liang, K. Wang, B. Cao, W. Zhu, H. Song, *Can. J. Chem. Eng.* **2017**, *95*, 2012.

[46] S. Ansaloni, N. Russo, R. Pirone, *Can. J. Chem. Eng.* **2017**, *95*, 1730.

[47] G. Yang, H. Chen, H. Qin, X. Zhang, Y. Feng, *Can. J. Chem. Eng.* **2017**, *95*, 1518.

[48] L. Wang, B. Shen, J. Zhao, X. Bi, *Can. J. Chem. Eng.* **2017**, *95*, 1069.

[49] C. J. Powell, M. P. Seah, *J. Vacuum Sci. Technol. A* **1990**, *8*, 735.

Manuscript received December 22, 2018; revised manuscript received April 10, 2019; accepted for publication April 10, 2019.